Journal of Hazardous Materials 211–212 (2012) 172–181

Contents lists available at SciVerse ScienceDirect

Journal of Hazardous Materials

journal homepage: www.elsevier.com/locate/jhazmat

Photocatalytic production of $^1O_2$ and •OH mediated by silver oxidation during the photoinactivation of *Escherichia coli* with TiO_2

Camilo A. Castro[a,b], Paula Osorio[b], Andrzej Sienkiewicz[c], Cesar Pulgarin[b,**], Aristóbulo Centeno[a], Sonia A. Giraldo[a,*]

[a] Centro de Investigaciones en Catálisis, Escuela de Ingeniería Química, Universidad Industrial de Santander (UIS), A.A. 678, Bucaramanga, Colombia
[b] Institute of Chemical Sciences and Engineering, GGEC, Swiss Federal Institute of Technology (EPFL), Station 6, CH-1015, Lausanne, Switzerland
[c] Laboratory of Complex Matter Physics, Institute of Physics of Condensed Matter, EPFL, Station 3, CH-1015, Lausanne, Switzerland

ARTICLE INFO

Article history:
Received 10 April 2011
Received in revised form 16 July 2011
Accepted 29 August 2011
Available online 3 September 2011

Keywords:
Ag–TiO_2
Hydrothermal synthesis
Visible light
EPR

ABSTRACT

Ag loaded TiO_2 was applied in the photocatalytic inactivation of *Escherichia coli* under ultraviolet (UV) and visible (Vis) light irradiations. Ag enhanced the TiO_2 photodisinfecting effect under Vis irradiation promoting the formation of singlet oxygen and hydroxyl radicals as identified by EPR analyses. Ag nanoparticles, determined on TEM analyses, undergo an oxidation process on the TiO_2's surface under UV or Vis irradiation as observed by XPS. In particular, UV pre-irradiation of the material totally diminished its photodisinfection activity under a subsequent Vis irradiation test. Under UV, photodegradation of dichloroacetic acid (DCA), attributed to photoproduced holes in TiO_2, was inhibited by the presence of Ag suggesting that oxidation of Ag^0 to Ag^+ and Ag^{2+} is faster than the oxidative path of the TiO_2's holes on DCA molecules. Furthermore, photoassisted increased of Ag^+ concentration on TiO_2's surface enhances the bacteriostatic activity of the material in dark periods. Indeed, this latter dark contact of Ag^+–TiO_2 and *E. coli* seems to induce recovering of the Vis light photoactivity promoted by the surface Ag photoactive species.

1. Introduction

TiO_2 photocatalysis has been subject of research interest as a promising technique to solve environmental problems, such as water disinfection and organic pollutants degradation [1–4]. The majority of efforts point to improve the TiO_2's photoactivity by increasing its photoresponse into the visible (Vis) part of the solar spectrum, and to decrease the recombination of the ultraviolet (UV) photogenerated charges, which are responsible of the generation of reactive oxygen species (ROS) in TiO_2 photocatalysis.

Ag modified TiO_2 photocatalysts have been synthesized using the hydrothermal method since this is a relatively simple route to load Ag onto TiO_2 nanoparticles [5,6], leading to well-dispersed Ag aggregates [5] and photoactive materials [7] with a wide range of optimum silver content from 0.1 to 6.5 wt% [8–10], correspondent to the major increase in photoactivity. Silver doping has been used to prop up Vis absorption [9,11,12]. The Ag loaded TiO_2 (Ag–TiO_2) spectral absorption covers a wider range than TiO_2, ranging from UV to Vis wavelengths up to 600 nm [11–13]. Ag^0 interactions with incident light enhance *Escherichia coli* photoinactivation activity of TiO_2 [8,13]. It has been proposed a decrease in recombination of the TiO_2 photogenerated charges that enhances the photocatalytic inactivation of *E. coli* due to Ag loading [13]. Moreover, Ag–TiO_2 antimicrobial activity was found to depend on the microbial strain, the Ag content and the Ag reducing agent used in the photocatalyst synthesis [8]. In addition, there has been a growing interest to develop antimicrobial devices containing silver for medical applications due to its bacteriostatic activity [14,15].

Furthermore, interesting optic characteristics of Ag–TiO_2 has been observed, such as multicolor photochromism, in which, electron transitions involving Ag and TiO_2 induce reductions and oxidations of the contained silver atoms [16,17], thus promoting different colors on the photocatalyst's surface [18,19]. Such electrons may also be transferred to O_2 [18], thus leading to a more efficient ROS production and to the higher TiO_2 photoactivity. However, the underlying mechanisms of such enhanced photoactivity are still under debate.

The aim of this study was to investigate the photocatalytic disinfecting activity of Ag–TiO_2 under Vis and UV irradiations. Results evidence that Ag loading remarkably increases TiO_2's photoactivity

* Corresponding author. Tel.: +57 7 6344746; fax: +57 7 6459647.
** Corresponding author. Tel.: +41 21 6934720; fax: +41 21 6935690.
E-mail addresses: cesar.pulgarin@epfl.ch (C. Pulgarin), sgiraldo@uis.edu.co, castro.lopezcamilo@gmail.com (S.A. Giraldo).

0304-3894/$ – see front matter © 2011 Elsevier B.V. All rights reserved.
doi:10.1016/j.jhazmat.2011.08.076

under Vis, which is related to singlet oxygen and hydroxyl radical generation, as observed by EPR spectroscopy.

2. Experimental

2.1. Photocatalysts synthesis

Photocatalysts were hydrothermal synthesized as follows: 3.8 mL of titanium isopropoxide (99.9%, Fluka) was added dropwise to 19 mL of isopropanol (Suprasolv. grade reagent, Merck). Then, an adequate amount of $AgNO_3$ (Extra pure, Merck) was diluted in 2 mL of water at pH 1.5 adjusted with HNO_3 (65%, Merck). Ag aqueous solution was added dropwise to the isopropoxide–isopropanol solution with an appropriate concentration to obtain Ag weight percentages (wt%), of: 0.4, 1.7 and 4.3. Formed gel was steam-pressure treated in autoclave during 3 h at 120 °C and ~144 kPa. TiO_2 was obtained as described without addition of $AgNO_3$ solution. The obtained wet crystals were grounded in mortar, dried in oven at 60 °C for 12 h, and kept in dark to avoid surface oxidation. Samples were labeled as: Ag(x)–TiO_2, x = Ag wt%.

2.2. Photocatalysts characterization

Fresh Ag(x)–TiO_2 and TiO_2 samples were XPS analysed. To follow Ag states after a typical photocatalytic test two 1 g/L Ag(1.7)TiO_2 suspensions, without *E. coli*, were submitted 2 h to Vis and UV irradiation, filtered and dried in oven at 60 °C and then XPS analysed. Analyses were carried out using an AXIS-NOVA photoelectron-spectrometer (Kratos-analytical, Manchester, UK) equipped with a monochromatic AlKα ($h\nu$ = 1486.6 eV) anode. Electrostatic-charge effect was overcompensated by means of the low-energy electron source working in combination with a magnetic immersion lens. C1s line at 284.8 eV was used as calibration reference. Spectra were decomposed using the CasaXPS program (Casa Software Ltd., UK) with a Gaussian/Lorentzian (70/30) product function after subtraction of a Shirley baseline. Assignment of Ag and Ti states was restricted using peak distances of 6 eV and 5.3 eV for Ag [13] and Ti [20], respectively.

X-ray diffraction (XRD) patterns were collected using a DMax-IIIB Rigaku system operated at room temperature, 40 kV and 80 mA with monochromatic Cu-Kα radiation. The average crystallite size (d_{XRD}) was calculated using the Scherrer equation applied to anatase peaks at 2θ = 25.2° on samples' diffractograms.

Diffusive reflectance spectroscopy (DRS) was done using a UV-2401PC Shimadzu spectrophotometer with an ISR240A integrating sphere accessory. $BaSO_4$ was used as reference.

Textural analyzes of the photocatalysts were performed through N_2 adsorption–desorption isotherms obtained at 77 K in a Nova1200 equipment of Quantachrome. Before the analysis 0.15–0.2 g samples were degasified during 12 h at 373 K under 10^{-5} mmHg vacuum. Specific surface area (S_{BET}), and average pore diameter (d_p) were obtained by means of BET and BJH methods, respectively. Transmission electrom microscopy (TEM) analyses were performed in a Phillips HRTEM CM 300 (field emission gun, 120 kV) microscope. TiO_2 and the 1.7 Ag loaded TiO_2 samples were chosen as representative materials for TEM analyses.

Reactive scavenging of ROS by electron paramagnetic resonance spectroscopy (EPR) was done using 2 mL of 0.3 g/L Ag(1.7)–TiO_2 suspension and 5×10^{-2} mol/L of the diamagnetic singlet oxygen scavenger 2,2,6,6-tetramethyl-4-piperidinol (TMP–OH, 99%, Fluka), with spectral parameters: DH = 1.58G, a_N = 16.9G, and g = 2.0066, was prepared in ultrapure H_2O, as well as, in D_2O (99.9% atomic purity, Aldrich). Suspensions were kept in test tubes and ultrasound treated in a water bath with a frequency of 40 kHz for 1 min prior to illumination. 1 mL aliquot of the suspension was transferred into a 5 mL Pyrex beaker and exposed to illumination under constant magnetic stirring with a white light halogen spot source of 150 W from OSRAM reference G×5.3 (93638) emitting Vis. ~7 μL aliquots of the illuminated suspensions were transferred into glass capillary tubes 0.7 mm ID and 0.87 mm OD, from VitroCom, NJ, USA. Tubes were sealed on both ends with Cha-Seal™ tube-sealing compound (Medex International, Inc. USA). To maximize sample volume in the active zone of the ESR cavity assemblies of seven packed capillaries were positioned in a wider quartz capillary (standard ESR tube, 2.9 mm ID and 4 mm OD, Wilmad-LabGlass, Vineland, NJ, USA). Such setup resulted in ~65 μL sample volume in the active zone of the ESR cavity, thus markedly improving sensitivity of measurements [21].

Experiments were performed using an ESR300 spectrometer (Bruker-BioSpin-GmbH) at room temperature, equipped with standard-rectangular mode TE_{102} cavity. Routinely, for each experimental point five scan field-swept spectra were recorded with instrumental parameters: microwave frequency: 9.38 GHz, microwave power: 2.0 mW, sweep width: 120G, modulation frequency: 100 kHz, modulation amplitude: 0.5G, receiver gain: 4×10^{-4}, time constant: 20.48 ms, conversion time: 40.96 ms, and time per single scan: 41.9 s. Acquired EPR traces correspond to the second derivative of the sample's paramagnetic absorption. A calibration point was made to correlate the double integrated signal, corresponding to the concentration, using a suspension of 100 mmol/L of fresh solution of a stable nitroxide radical, 4-hydroxy-2,2,6,6-tetramethylpiperidine 1-oxyl (TEMPOL, Sigma–Aldrich).

Ag contents were established by Flame atomic absorption spectrometry (FAAS) in a Buck-Scientific 210VGP spectrometer using 6.4 g of $(NH_4)SO_4$ and 16 mL of concentrated H_2SO_4 added to 0.2 g of the photocatalyst sample. The suspension was heated at 80 °C under vigorous agitation until complete dissolution, and then cooled and diluted in distilled water for absorption measurements.

2.3. Photocatalytic activity

Photocatalytic tests were done using Pyrex bottles (50 mL) with aqueous suspension of *E. coli*, or dichloroacetic acid, and 1 g/L of TiO_2. Suspensions were kept under magnetic stirring and illuminated under two different lamp set-ups: (I) 38 W/m^2 of UV using a set of 5 BLB-Phillips lamps (TLD 18 W) with emission between 330 and 400 nm, or, (II) 60 W/m^2 of Vis using a set of 5 Blue-Phillips lamps (TLD 18 W) with emission between 400 and 500 nm. Radiant flux was monitored with a Kipp&Zonen CM3 power meter (Omni-instruments Ltd., Dundee, UK).

Photobactericidal activity was measured by sampling *E. coli* strain K12-MG1655 from photoreactors. Before experiments, bacteria were inoculated into Luria Bertani growth media (1 wt%, Tryptone from Oxoid, 0.5 wt% yeast extract from Oxoid, and 1 wt% NaCl from Merck) and grown during 8 h at 37 °C. During the stationary growth phase, bacteria were harvested by centrifugation at 5000 rpm for 10 min at 4 °C. The obtained bacterial pellet was washed three times with saline solution (8 g/L NaCl, 0.8 g/L KCl in Milli-Q water, pH 7 by addition of HCl or NaOH). A suitable cell concentration (10^7 colony forming units (CFU)/mL) was inoculated in the reactor's saline solution. Then, 0.05 g of photocatalyst was added to each reactor. Suspensions were illuminated during 2 h and samples (1 mL) were taken at different time intervals. Serial dilutions were performed in saline solution and 10 μL samples were inoculated 4 times in plate count agar (PCA, Merck). The number of colonies was counted after 24 h of incubation at 37 °C.

DCA photodegradation was done using concentrations of 130 mg/L DCA and 1 g/L of Ag(1.7)TiO_2 as recommended to follow the kinetics on DCA photooxidation by TiO_2 holes [22]. Samples were taken and filtered using 0.2 μm membranes. DCA

concentration was followed by HPLC analysis with a Hewlett-Packard 1100 equipment using a Supelcogel-H column at 60 °C. H_2SO_4 5×10^{-3} mol/L solution was used as mobile phase. Detection was done by a refractive index detector.

Data hereby reported is expressed as C/C_0, where C = DCA molar concentration. Initial concentration (C_0) is the concentration reached in the suspension after 1 h of stirring prior illumination.

Ag leaching from the Ag(1.7)TiO_2 sample was determined in a UV irradiated suspension of the photocatalysts without the addition of *E. coli* to avoid interference due to Ag absorption by bacteria. The irradiated suspension was filtered using a 0.45 μm-membrane and Ag was determined using: (i) FAAS after the irradiation period. And, (ii) adding 5 mL of a 0.1 mol/L NaOH to observe AgCl precipitation.

2.4. Pre- and post-irradiation experiments

Pre-irradiation experiments were carried out to understand the effect of previous irradiations on Ag–TiO_2 photoactivity. Two 1 g/L Ag(1.7)TiO_2 suspensions were irradiated; one under Vis, and the other under UV during 4 h. Then, a suitable aliquot of *E. coli* suspension was added to the photocatalyst suspension and irradiated under Vis for 2 h. Samples were taken at different time intervals.

Two post-irradiation experiments were made, one after the other. Ag(4.3)TiO_2 was used to increase Ag concentration on the photocatalyst surface to analyse its bacteriostatic activity under dark-contact with *E. coli*. First, to evaluate the effect of UV pre-irradiation on the Ag(4.3)TiO_2 bacteriostatic activity an experiment in dark was done, in which *E. coli* was added to a 10 h UV pre-irradiated Ag(4.3)TiO_2 suspension. This suspension (*E. coli* + UV-pre-irradiated Ag(4.3)TiO_2) was constantly stirred during another 10 h. Samples were taken in time intervals of 2 h. This used photocatalyst suspension will be referred as "used-in-dark". For comparison purposes fresh Ag(4.3)TiO_2 was suspended and evaluated in darkness using the described procedure. Second, to evaluate possible changes in photoactivity due to the described dark processes the used-in-dark suspension was evaluated towards *E. coli* photoinactivation under Vis. In this case, *E. coli* was added to the used-in-dark Ag(4.3)TiO_2 suspension after the described 10 h dark process and further submitted to Vis for 3 h. Samples were taken at different time intervals. The correspondent blank experiment using the used-in-dark Ag(4.3)TiO_2 was made in darkness to evaluate the remain bacteriostatic activity after the former dark process.

Moreover, to analyse the bactericidal activity of Ag^+ ions in solution (lixiviation) an Ag(4.3)TiO_2 suspension was stirred under darkness for 10 h and then filtered. *E. coli* was added to the filtered solution, and bacteria concentration was determined at intervals of 2 h and under darkness. Since *E. coli* is inactivated by Ag^+ ions in solution it is possible then to determine if lixiviated Ag may decrease bacteria concentration [26].

3. Results

3.1. Photocatalyst characterization before and after UV and Vis irradiations

Ag(1.7)TiO_2 and TiO_2 X-Ray diffractograms are shown in Fig. 1. Anatase is identified as the primary crystalline phase in both samples with peaks at 2θ of 25.2°, 37.9°, 48.2°, 55.0° and 62.6°. Since, Ag^+ and Ti^{4+} ionic radii are 1.16 [23] and 0.64 Å [24], respectively, is not expected that Ag may be embedded into the TiO_2 structure but onto the surface. However, low concentrations did not allow to identify Ag phases in XRD analyses.

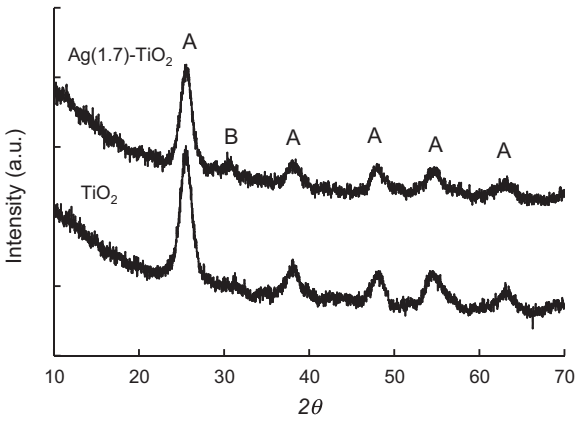

Fig. 1. X-Ray diffractograms of TiO_2 and Ag(1.7)–TiO_2 samples. A:anatase, B:brookite.

Table 1 shows calculated average crystallite size of the samples, their textural properties; S_{BET} and d_p, and its elemental composition. As observed there were no significant changes in crystallite size due to Ag loading, but instead, it was possible to observe a decrease in anatase crystallinity since the peak at 25.2° of Ag(1.7)TiO_2 (Fig. 1) is wider and shorter than that of TiO_2. In addition, a slight peak at 30.7° of brookite is observed for Ag(1.7)TiO_2.

Moreover, textural properties observed in Table 1 evidence that hydrothermal synthesis leads to a high S_{BET} mesoporous particles with a ~7% decrease of TiO_2 surface when loading with 4.3 wt% of Ag, moreover, the average pore diameter was reduced in a similar extent.

Table 1 shows the elemental composition as E/Ti ratios, with E = Ag, C or O. As observed, Ag/Ti and C/Ti ratios, determined on XPS analyses, are reduced by action of the irradiation periods suggesting a slight lixiviation of Ag aggregates with either light source; UV or Vis, and surface oxidation processes that decrease carbon–organic residues on the surface, respectively. Furthermore, additional changes are observed on the XPS spectra of the samples. Ag lixiviation was determined after UV irradiation and was not detected by FAAS. In agreement to this, AgCl precipitation was not observed after addition of a 1 N NaOH solution, thus confirming that Ag lixiviation is low.

Fig. 2 shows the Ag3d XPS spectra of the fresh and the UV and Vis irradiated Ag(1.7)TiO_2. Fresh Ag(1.7)TiO_2's spectrum (Fig. 2a) shows two individuals peaks at 374.6 and 368.5 eV assigned to $Ag3d_{3/2}$ and $Ag3d_{5/2}$, respectively. After peak deconvolution it is observed the presence of two different peaks for $Ag3d_{5/2}$,: one at 368.4 eV assigned to Ag^+ [13,25], while the peak at 368.7 eV is attributed to Ag^0 [13,26]. Thus, results suggest the coexistence of Ag_2O and Ag^0 probably due to the oxidative action of isopropanol on Ag^+ ions [27] during the synthesis process.

Vis (Fig. 2b) and UV (Fig. 2c) irradiated samples' spectra show a positive shift of 1.1 and 1.4 eV, respectively, positioning $Ag3d_{5/2}$ at 367.5 eV, and $Ag3d_{3/2}$ at 373.5, for the Vis irradiated sample, and $Ag3d_{5/2}$ at 367.2 eV and $Ag3d_{3/2}$ at 373.2 eV, for the UV irradiated one. This suggests a decrease in Ag reduced species content for the Vis irradiated sample and the formation of Ag^+ as Ag_2O and Ag^{2+} as AgO [28]. It was not possible to assign an additional peak for Ag^+ for the UV irradiated sample. Instead, it is observed a peak assigned to Ag^{2+} at 367.2 eV. Hence, Ag^0 concentration has remarkably decreased during irradiation (either Vis or UV) of Ag(1.7)TiO_2 increasing the signals of the Ag oxidized states with a more notorious oxidative effect due to UV.

Fig. 3 shows the Ti2p XPS spectra of TiO_2 (Fig. 3a) and Ag(1.7)TiO_2 (Fig. 3b). Ti2p spectrum is formed by two peaks at:

Table 1
Textural properties and XPS-determined elemental composition of TiO_2 and Ag modified TiO_2 samples.

Samples		Crystallite Size	Textural properties		Elemental composition[a]		
		d_{XRD} (Å)	S_{BET} (m^2/g)	d_p (Å)	Ag/Ti	C/Ti	O/Ti
TiO_2		50.4	230	26.53	–	0.870	2.890
Ag(1.7)TiO_2	Fresh	49.9	224	22.67	0.028	0.936	2.598
	UV treated	–	–	–	0.017	0.492	2.671
	Vis treated	–	–	–	0.021	0.519	3.057
Ag(4.3)TiO_2		49.5	215	24.42	0.033	0.958	2.660

d_{XRD}: Average crystallite size; S_{BET}: specific surface area, d_p: average pore diameter.
[a] XPS determined.

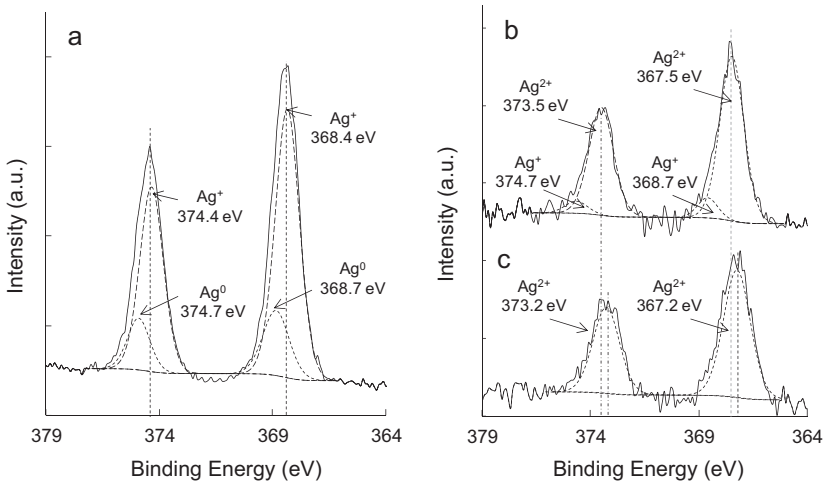

Fig. 2. XPS Ag 3d spectra of the: (a) fresh, (b) Vis, and (c) UV irradiated Ag(1.7)–TiO_2 samples.

458.9 eV and 464.55 eV, assigned to $Ti2p_{3/2}$ and $Ti2p_{1/2}$, respectively, indicating a predominant state of Ti^{4+} [29]. Moreover, no shift was found for Ti2p in Ag loaded TiO_2's spectrum suggesting the absence of Ag–Ti chemical bonds. As observed in Fig. 3c, Vis light did not change the spectrum of the fresh Ag(1.7)TiO_2 sample, while UV (Fig. 3d) induced: the reduction of the Ti^{4+} signal intensity at 458.9 eV, the formation of a second peak at 457.9 eV assigned to Ti^{3+} [30], and a shift of the $Ti2p_{1/2}$ peak by 1.1 eV due to the formation of the Ti^{3+} doublet (not shown). Therefore, UV induces dramatic changes in the surface chemical composition of Ag(1.7)TiO_2 that are expected to have an important effect on photoactivity.

DRS spectra of the photocatalysts are shown in Fig. 4. TiO_2 spectrum consists of a wide absorption band below ~370 nm ascribed to electron transitions from the valence band (VB), to the conduction band (CB) [31]. Moreover, an interesting light response was found for Ag loaded samples. Increase in Ag concentration induces a shift in light absorption to the Vis range for wavelengths up to 800 nm. In addition, the 4.3% Ag loaded sample shows a shoulder-like peak at ~490 nm, which has been proposed for Ag^0 nanoparticles inducing

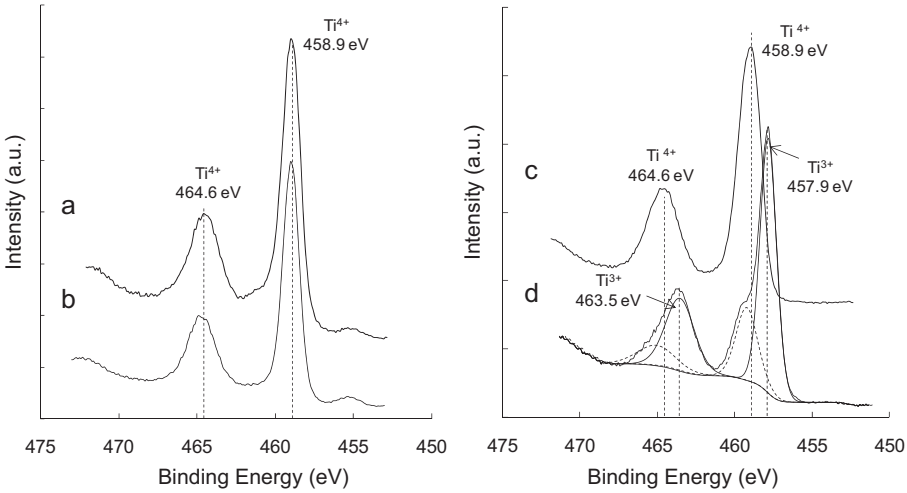

Fig. 3. XPS Ti2p spectra of the (a) TiO_2 and (b) fresh, (c) UV, (d) Vis irradiated Ag(1.7)–TiO_2 samples.

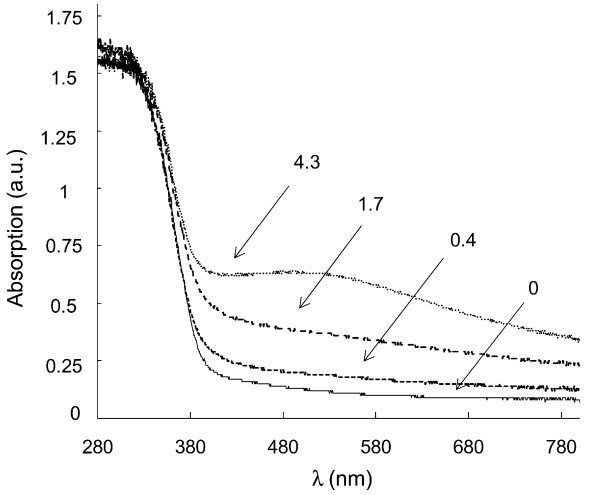

Fig. 4. DRS spectra of the Ag(x)–TiO_2 samples, with x = 0, 0.4, 1.7 and 4.3Ag nominal wt%.

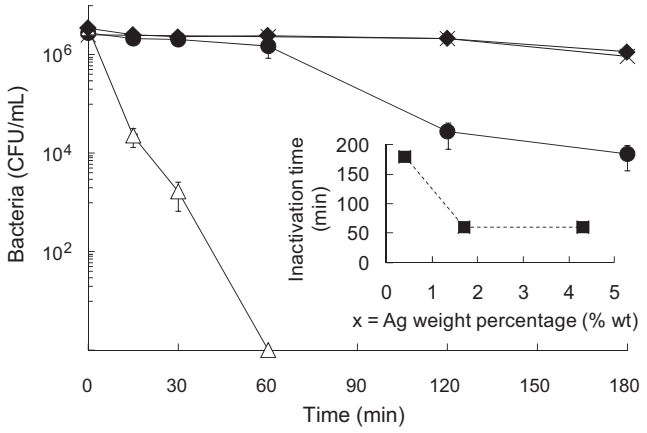

Fig. 6. *E. coli* photocatalytic inactivation under Vis by (Δ) Ag(1.7)–TiO_2, (●) TiO_2, (×) light blank, and, (♦) Ag(1.7)–TiO_2 under dark. Inset: time needed for total inactivation by the Ag(x)–TiO_2 photocatalysts.

Vis light absorption [17]. Additionally, $Ag_n^{\delta+}$ clusters (where n is in the range 2–13, and $\delta = n - 1$, with $n > 3$) present three absorption bands at 360, 460 and 500 nm [32]. Bands at 350–380 nm are attributed to Ag clusters of ~1 nm size, while clusters of 10 nm size and crystallites absorb at 400–500 nm [32,33], as in our case. TEM micrographs of the TiO_2 and Ag(1.7)TiO_2 samples are shown in Fig. 5. The TiO_2 sample is constituted of irregular particles with approximate sizes of 8–10 nm. Difference between dXRD and the observed particles size in TEM analysis is due to agglomeration of crystallites. In addition, the Ag(1.7)TiO_2 micrograph shows a similar size distribution to that of bare TiO_2. Previously suggested ~5 nm Ag nanoparticles are observed on the TiO_2 surface thus confirming that the hydrothermal synthesis promotes loading of Ag aggregates on TiO_2 due to the above discussed difference in atomic radii. Therefore, results suggest that partially oxidized AgO nanoparticles were deposited on TiO_2 surface during photocatalyst synthesis inducing remarked effects on its absorption properties.

3.2. Photocatalytic inactivation of E. coli

Fig. 6 shows the results of water photodisinfection using Ag(x)TiO_2 and TiO_2 under Vis. Inset shows the required time for total disinfection using Ag(x)TiO_2 samples. Ag(1.7)TiO_2 completes total inactivation within the first 60 min of Vis irradiation while TiO_2 shows a lower photoactivity. Blank experiments using the Ag(1.7)TiO_2 sample under dark, and without photocatalyst under Vis, suggest absence of: (i) photocatalyst toxicity, and (ii) photodisinfection effect of the Vis light source during the irradiation time. In addition, as observed in the inset, there is an increase in TiO_2 Vis light photoactivity when increasing Ag concentration up to 1.7 wt%, after which there seems to be no increase in photoactivity. Xin et al. [9] observed a decrease in photoactivity after 5 mol percentage (6.6 wt%) of Ag loading and proposed that excess Ag act as a recombination center and decreases TiO_2's light absorption capacity.

Fig. 7 shows the photodisinfection performance of Ag(1.7)TiO_2 and TiO_2 under UV. Ag(1.7)TiO_2 performance was similar to that of TiO_2, hence, UV irradiation does not photoactivate Ag–TiO_2 to promote *E. coli* inactivation.

Commercial TiO_2 Degussa P25 was tested at the reaction conditions of experiments observed in Figs. 6 and 7. Results showed zero photoactivity towards *E. coli* inactivation for P25 while under UV irradiation photoactivity was similar to that of the TiO_2 sample, thus confirming the high performance of our material in water photodisinfection processes.

Furthermore, Fig. 8 shows the photodisinfection activity under Vis of Ag(1.7)TiO_2 samples that were pre-irradiated for 2 h under Vis and UV, and for comparison; the fresh sample. As observed, the UV pre-irradiated sample has totally diminished its photoactivity

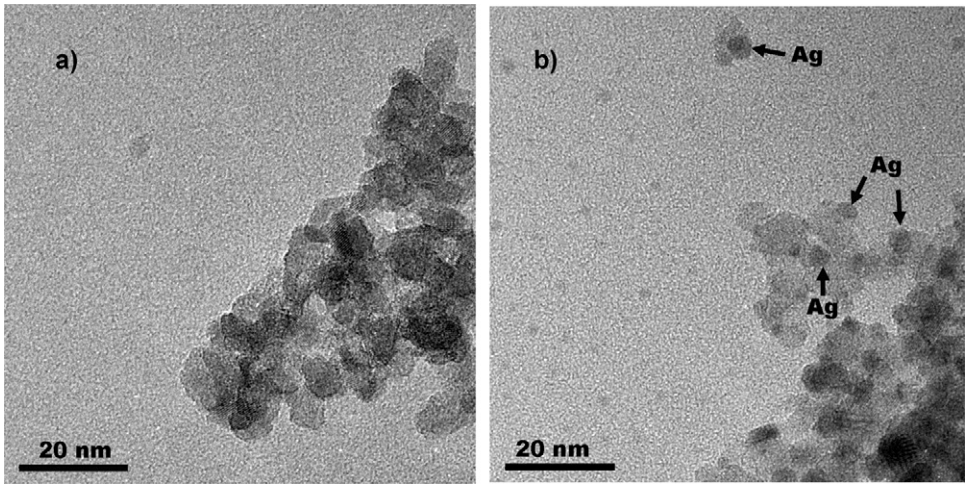

Fig. 5. TEM micrographs of the a) TiO_2 and the Ag(1.7)TiO_2 samples.

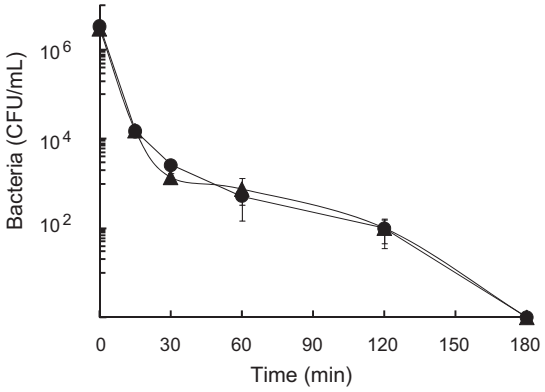

Fig. 7. *E. coli* photocatalytic inactivation under UV using: (▲) Ag(1.7)–TiO_2, and, (●) TiO_2 samples.

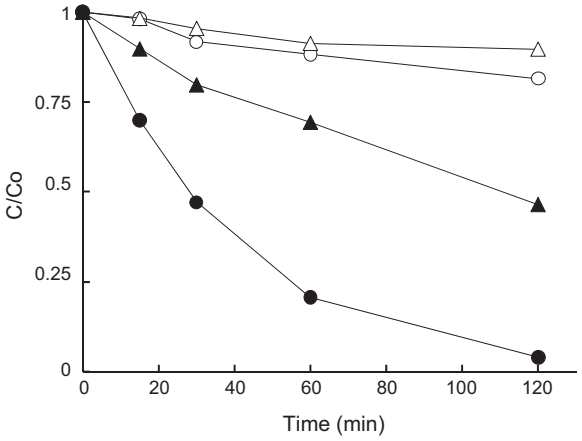

Fig. 9. DCA photocatalytic degradation using Ag(1.7)–TiO_2: under visible (△) and ultraviolet (▲) irradiations, and TiO_2 under Vis (○) and UV (●) irradiations.

under Vis, while the Vis pre-irradiated sample has a similar performance to that of the fresh one.

3.3. Photocatalytic degradation of dichloroacetic acid (DCA)

Fig. 9 shows the performance of Ag(1.7)TiO_2 and TiO_2 on the DCA photodegradation under Vis and UV. Vis did not induce DCA photocatalytic degradation using either of the samples, while TiO_2 has a better performance than Ag(1.7)TiO_2 under UV suggesting a reduction in photoactivity due to Ag loading.

Formation of AgCl precipitates due to the observed minimum Ag lixiviation (Table 1) and Cl^- presence, by dissolution of NaCl (during photodisinfection tests) or DCA, is probably promoted. However, this phenomena did not generate any toxicity of the photocatalysts as observed for the fresh Ag(1.7)TiO_2 sample, and since its formation do not depend on irradiation this would not have any effect on photoactivity.

3.4. ROS identification under Vis irradiation

ROS formation, such as, singlet oxygen ($^1O_2$) and hydroxyl (•OH) radicals was monitored by EPR. It is well known that non-paramagnetic TMP–OH (nitroxide precursor) reacts with $^1O_2$, thus forming the paramagnetic product TEMPOL, which can easily be followed by EPR detection [34,35]. Fig. 10 shows the reached TEMPOL concentration after 100 min of Vis irradiation of TiO_2 and Ag(1.7)TiO_2 suspensions in D_2O. $^1O_2$ formation was clearly evidenced for Ag(1.7)TiO_2 with a characteristic 1:1:1 triplet signal of TEMPOL as depicted in the inset to Fig. 10. In addition, Ag doped sample revealed an increase in $^1O_2$ photoproduction in comparison to TiO_2.

Moreover, new ROS were detected using H_2O as solvent. Fig. 11 shows the EPR signal obtained after 120 min of Vis irradiation of Ag(1.7)TiO_2 suspensions using D_2O and H_2O, the inset depicts the difference between the signals obtained using different solvents. A higher signal intensity was observed for Ag(1.7)TiO_2 than that obtained with TiO_2, both irradiated with Vis light.

It is well known that $^1O_2$ lifetime increases in D_2O, which usually leads to reaction rate enhancement of $^1O_2$-mediated processes. Therefore, in the context of $^1O_2$ reactive scavenging, using TMP–OH, such D_2O-isotope effect should result in increasing the EPR-detected TEMPOL signal [34–36]. Though, in our case, there was a reversed isotopic effect since the signal obtained in H_2O shows a higher intensity in comparison to that obtained using D_2O. Furthermore, an additional EPR signal, with spectral parameters: of DDH = 0.47G, a_N = 15.9G, g = 2.0065, was observed. This signal, overlaps with the TEMPOL signal for the irradiated Ag(1.7)TiO_2 aqueous suspension, and corresponds to another nitroxide radical; TEMPONE, which is a product of •OH attack to TEMPOL [37]. Therefore, the overall reduced rate of TEMPOL formation in D_2O is probably due to lower quantum efficiency of D_2O photocatalytic oxidation to form ROS, such as, "*deuteroxyl radicals*", by TiO_2 [38].

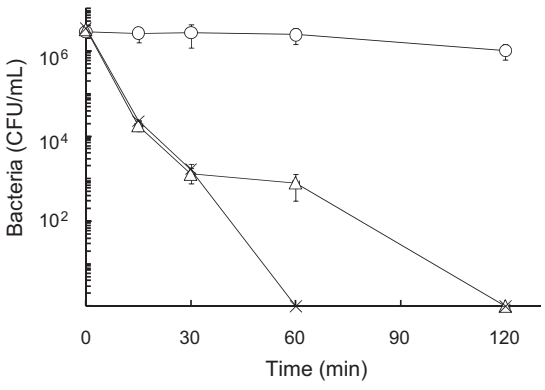

Fig. 8. *E. coli* photocatalytic inactivation using the fresh Ag(1.7)–TiO_2 (×), and the pre-irradiated Ag(1.7)–TiO_2 under Vis (△) and UV (○) irradiations.

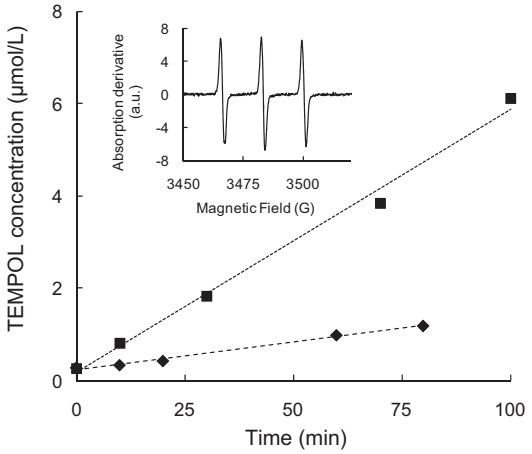

Fig. 10. . Photocatalytic TEMPOL productionsusing: (■) Ag(1.7)–TiO_2, and, (♦) TiO_2 samples. Inset: the characteristic triplet signal obtained for TEMPOL using the Ag(1.7)–TiO_2 irradiated for 100 min under Vis.

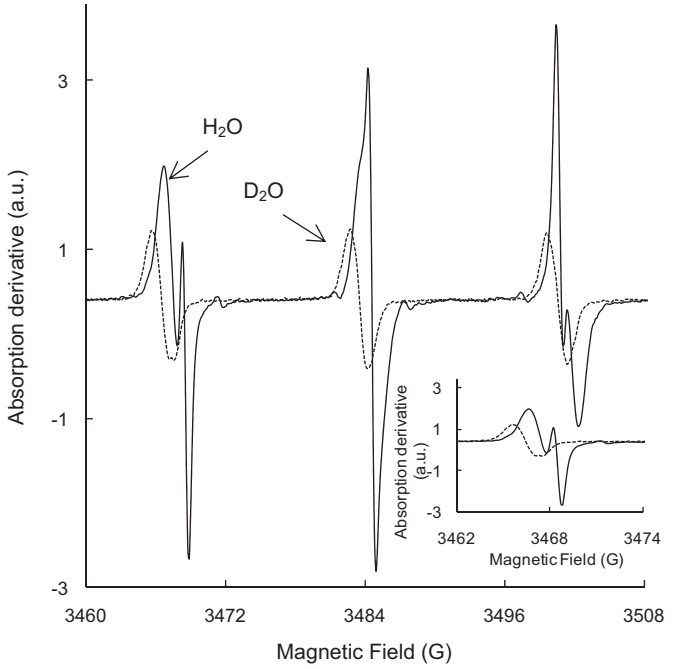

Fig. 11. EPR spectra of the aqueous and deuterium suspensions of Ag(1.7)–TiO_2 and TMP–OH after 120 min of Vis irradiation. Inset: magnification of the absorption derivative signal between 3462 and 3474G.

3.5. Post-irradiation events in darkness and under Vis

Fig. 12a shows the behavior of *E. coli* in dark contact with two samples of Ag(4.3)TiO_2; the 10 h UV pre-irradiated sample, and the fresh one. The fresh Ag(4.3)TiO_2 sample did not reduce *E. coli* concentration during 10 h of dark suspension. On the contrary, UV pre-irradiated Ag(4.3)TiO_2 could initiate an effective disinfection after 4 h of dark suspension leading to a total decrease in *E. coli* concentration in 8 h.

Fig. 12b shows the performance of the used-in-dark Ag(4.3)TiO_2 sample in *E. coli* photoinactivation under Vis. This sample completed inactivation within 60 min. As previously noted, UV pre-irradiation leads to a total decrease in photoactivity (Fig. 8), while in this case, Vis irradiation promoted total *E. coli* inactivation within 60 min, thus suggesting a regaining of the surface photoactivity of the UV-treated Ag(4.3)TiO_2 sample due to the dark contact with *E. coli*. In addition, this sample maintained its bacteriostatic activity and totally inactivated bacteria in 3 h under dark (Fig. 12b).

4. Discussion

4.1. Ag loading effect on TiO_2 photoactivity under UV and Vis irradiations

Characterization showed that Ag–TiO_2 is constituted by anatase as major constituent phase (Fig. 3) with Ag nanoparticles on its surface formed by Ag^0 and Ag^+ species (Fig. 1). In addition, Ag(1.7)TiO_2 XRD diffractogram evidenced brookite formation due to Ag loading. Ag doping decreases the temperature in which the anatase–rutile transition occurs by decreasing the boundary energy due to Ag aggregates located in crystals borders [39,40], therefore, lower energy is required for such transformation. In fact, a similar effect, by Ag-boundary located aggregates, may be promoted in our case since the anatase to brookite transformation is energetically low (11.9 kJ/mol [41]). And, as it was observed also decreases the specific surface area [42] and the average pore diameter by distorting the distribution of the mesoporous structure, blocking it by deposition during the synthesis process.

The lack of a calcination step seems to promote amorphicity of the samples evidenced on wideness and low definition of anatase and brookite peaks. However, a TiO_2 material obtained using the same synthesis route showed a similar performance than that of the commercial TiO_2-P25 towards azo dye photocatalytic degradation [3]. In addition, amorphous Fe and Cr doped TiO_2 showed a significant increase in photoactivity in comparison to bare TiO_2 particles, which indeed maintained its photoactivity after several uses [43]. Therefore, amorphicity of the TiO_2 and Ag loaded TiO_2 samples seem not to decrease photoactivity.

Moreover, DRS analyses showed an increase in TiO_2 Vis light absorption with a shoulder-like peak due to Ag presence. Such response has been observed for Ag-nanometric particles deposited on TiO_2 surface presenting a surface plasmon resonance (SPR) effect in which CB electrons are collectively excited by certain Vis-light wavelengths [17], which in our case seems to be at ~490 nm [11,13]. This extended absorption indicates that surface Ag give rise to new energy levels promoting lower energetic transitions.

Ag(1.7)TiO_2 sample with Ag^0 and Ag^+ species showed an increase in *E. coli* photoinactivation under Vis. However, under UV irradiation the performance of the Ag(1.7)TiO_2 sample was similar to that of TiO_2. Such features seem to be determined by Ag^0 and Ag^+ species in the Ag(1.7)TiO_2's surface. Indeed, UV pre-irradiation remarkably decreased concentration of the Ag^0 and Ti^{4+} species (Figs. 1 and 2), process related to a total decrease in photoactivity as observed in Fig. 8. Hence, results point Ag^0 to Ti^{4+} interaction, promoted under Vis, as a determinant process in photoactivity.

Moreover, as it was observed in XPS analyses, C/Ti ratio was observed to decrease after irradiation periods thus suggesting

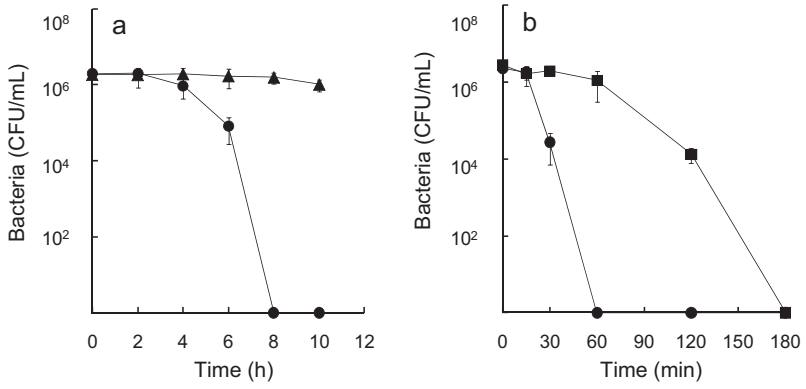

Fig. 12. Post-irradiation events using Ag(4.3)–TiO_2 in contact with *E. coli* suspensions. (a) Under dark using: (▲) fresh and (●) UV pre-irradiated samples. And, (b) photoactivity of the used-in-dark sample under: (●) Vis and, (■) in darkness as reference.

oxidation of organic residues coming from the synthesis procedure that could compete for ROS. Nevertheless, since photodisinfection activity under Vis was not observed to decreased it is possible to reject ROS, or charge, trapping by such organic residues when using the Ag(1.7)TiO_2 sample.

Analysis of DCA photodegradation (Fig. 9) showed contrary results for Ag(1.7)TiO_2 photoactivity. After adsorption on TiO_2's surface, DCA oxidation occurs due to photoproduced holes (h^+_{VB}) by UV excitation [22,44]. In our case, Vis did not promote DCA degradation using any of the samples. Probably, Ag could not promote charge separation under Vis, and thus, there were no available h^+_{VB} to oxidize DCA. In fact, under UV irradiation there was a decrease in photoactivity due to Ag loading. Hence, it is possible that photoproduced h^+_{VB} (Eq. (1)) are being hindered from their oxidative action on DCA by Ag, and thus, h^+_{VB} oxidize more rapidly Ag^0 to Ag^+ and Ag^{2+} (Eqs.(2) and (3)) than DCA adsorbed molecules. In addition, stabilized holes leave free UV photogenerated electrons that may be responsible of Ag(1.7)TiO_2 *E. coli* photoinactivation activity under UV by inducing formation of ROS, and thus, reaching TiO_2 photoactivity (Fig. 5).

$$TiO_2 + h\nu(\lambda < 400\,nm) \rightarrow h^+_{VB} + e^-_{CB} \quad (1)$$

$$Ag^0 + h^+_{VB} \rightarrow Ag^+ \quad (2)$$

$$Ag^+ + h^+_{VB} \rightarrow Ag^{2+} \quad (3)$$

Ag^0 oxidation by TiO_2 has been reported. The increased thickness of a Ag_2O film by Ag^0oxidation was suggested to be induced under irradiation in the interface of a TiO_2–Ag^0 thin film [45]. Moreover, gold and silver, showing the SPR effect induced by Vis excitation, have been proposed to induce transport of electrons to TiO_2, thus leaving Au and Ag as positive charged ions [17]. Such oxidation processes are thermodynamically possible since Ag^+/Ag^{2+} and Ag^0/Ag^+ electrochemical potentials (1.98 and 0.799 V vs SCE [46], respectively) lie between the CB and VB energy levels (−0.2 and 3.0 V vs SCE, respectively [1]) of TiO_2. Plus, to complement the redox process it is possible to note that electrons released from Ag^0 oxidation induce reduction of Ti^{4+} to form Ti^{3+}.

Therefore, since Vis irradiation did not increase Ag(1.7)TiO_2 photoactivity towards DCA degradation (Fig. 9), Vis-activated Ag^0 particles seem not to be related to charge separation but to an increase in *E. coli* photoinactivation.

Indeed, visible performance of modified TiO_2 photocatalysts has been previously observed to be higher than under UV irradiation. It has been reported by Rengifo-Herrera et al. [47] that modification with nitrogen and sulfur coming from thiourea decomposition over TiO_2 surface increase the response of the material towards visible irradiation, indeed, such modification led to a worse performance under UV irradiation. Moreover, it has been recently reported that transition metal ions, such as Fe, induce recombination of TiO_2's photogenerated charges leading to a decrease in photoactivity under UV irradiation [48]. Thus, this partially confirmed the suggested above since in this case Ag did not promote photoactivity under UV irradiation due to charge trapping. However, before proposing a new mechanism of light activation it is necessary to clarify the production of ROS under Vis.

4.2. Mechanism of ROS production during Ag–TiO_2 Vis irradiation

Zhang et al. [49] proposed a Rose Bengal induced $^1O_2$ formation process enhanced by a SPR effect induced on silver particles' surface. In addition, Shcherbakov et al. [50] reported a mechanism in which metal oxides embedded in a semiconductor matrix, such as; V_2O_5/SiO_2 and MoO_3/SiO_2 photogenerated certain amounts of $^1O_2$ when irradiated with a mercury lamp. Then, illumination of the oxide generates an intermediate metallic oxide complex; $(Mo^{5+}–O^-)^*$, that promotes $^1O_2$ photogeneration in presence of O_2 (Eq. (4)) and a further regeneration of the initial chemical state of molybdenum.

$$(Mo^{6+} = O^{2-}) + h\nu \rightarrow (Mo^{5+}O^-)^* \rightarrow (Mo^{5+} - O^-)^* + O_2 \rightarrow (Mo^{6+} = O^{2-}) + {}^1O_2 \quad (4)$$

In their study Shcherbakov et al. did not evidence surface chemical states of the irradiated sample to confirm the return of the initial Mo^{6+} state. Therefore, in our case it is possible to suggest that $^1O_2$ formation is promoted by Vis excited Ag species on the TiO_2's surface (Eq. (5)), thus, promoting electrons to the CB of TiO_2 and Ag^+ formation. Finally, the CB electron (e^-_{CB}) is transferred to adsorbed O_2 molecules promoting $^1O_2$ generation, Eq. (6). Such energy transfer to O_2 has also been suggested using a hypocrellin B–chelated TiO_2 [51].

$$Ag^0 - TiO_2 + h\nu(\lambda > 400\,nm) \rightarrow Ag^+ - TiO_2(e^-_{CB}) \quad (5)$$

$$Ag^+ - TiO_2(e^-_{CB}) + O_2 \rightarrow {}^1O_2 \quad (6)$$

$^1O_2$ attack is responsible for *E. coli* inactivation in Vis irradiated Ag–TiO_2 suspensions since, as it is well known, a vast majority of cell types, from prokaryotic to mammalian, undergo irreversible damage leading to cell death by exposure to $^1O_2$ [35,52,53].

Nevertheless, •OH was also detected in EPR experiments during Vis irradiation (Fig. 11). Probably, •OH formation in H_2O may be induced by electron transfer between the Vis excited Ag^0 particles and the CB of TiO_2. A possible route for •OH formation is through chain reactions (Eqs. (8)–(11)) that may be started by the superoxide radical ($O_2^{\bullet -}$) [1] involving O_2 and the TiO_2's e^-_{CB}, Eq. (7).

$$O_2 + e^-_{CB} \rightarrow O_2^{\bullet -} \quad (7)$$

Then, $O_2^{\bullet -}$ dismutation promotes H_2O_2 formation,

$$O_2^{\bullet -} + H^+ \rightarrow HO_2^{\bullet -} \quad pK_a = 4.88 \quad (8)$$

$$HO_2^{\bullet} + HO_2^{\bullet} \rightarrow H_2O_2 + O_2 \quad (9)$$

$$H_2O_2 + e^-_{CB} \rightarrow {}^{\bullet}OH + OH^- \quad (10)$$

$$H_2O_2 + O_2^{\bullet -} \rightarrow {}^{\bullet}OH + OH^- + O_2 \quad (11)$$

$O_2^{\bullet -}$ production may be enhanced by e^- transfer from excited Ag^0 particles to TiO_2's CB. But, since pH of the Ag–TiO_2 suspension is 6.5 it seems not to be possible •OH generation through $O_2^{\bullet -}$ dismutation (pK_a = 4.88). Even so, Okuno et al. [54] reported the enhanced •OH formation from $O_2^{\bullet -}$ using organic selenium compounds in a pH 7.4 media. In this case, selenium compounds acted as electron donors in a dismutation reaction forming H_2O_2 from $O_2^{\bullet -}$. Then, surface e^- availability on Vis irradiated Ag–TiO_2 would probably induce $O_2^{\bullet -}$ dismutation explaining •OH formation, which in joint action with $^1O_2$, effectively inactivates *E. coli*. In addition, it has been recently observed that Gram-positive bacteria are efficiently inactivated by $O_2^{\bullet -}$ action, while Gram-negative are inactivated by •OH action [55]. Therefore, it is possible to expect prospect findings, using Ag–TiO_2 photocatalyst towards bacteria with different wall structures.

4.3. Ag-oxidized species content effect on Ag–TiO_2 bacteriostatic activity in post-irradiation events

Post-irradiation experiments showed an interesting performance of the Ag–TiO_2 sample in dark contact with *E. coli*. As observed, the UV treated Ag–TiO_2 sample increased its bacteriostatic activity (Fig. 12a) in dark periods. Furthermore, this dark contact promoted photoactivity in a subsequent *E. coli* photoinactivation test done under Vis (Fig. 12b). For that reason, it is possible to

suggest that in darkness the bacteria's outer membrane may act as electron donors probably regenerating the Ag^0 species needed for a further photoactivation and production of ROS under Vis. Probably, these suggested electron transfer may cause the oxidation of *E. coli*'s cell wall, perhaps explaining its inactivation in darkness.

The evolution of the *E. coli* concentration added to a filtered solution of a 10 h-dark-stirred Ag(4.3)TiO_2 suspension showed that bacteria decreased to $\sim 2 \times 10^5$ CFU/mL after 10 h of dark suspension of the filtered solution. This suggests that Ag^+ ions have been released, from the photocatalyst's surface during the dark-stirring process, and after filtration may induce toxicity leading to bacteria death. However, total inactivation was not reached thus confirming that toxicity observed during dark contact of *E. coli* with UV-pre-irradiated Ag(4.3)TiO_2 (Fig. 12a) is mostly due to heterogeneous contact with the photocatalyst's surface. However, further studies should be done to understand lixiviation processes in post-irradiation events.

In addition, after three consecutive uses of the Ag(1.7)TiO_2 sample (results not shown), in which *E. coli* was added after 2 h of solar-simulated light irradiation (samples taken at the beginning and end of each irradiation period), the photocatalyst maintained its photoactivity and zero bacteria counting was found after the reuse testing. Thus, to discuss the stability of the material it is important to highlight: (i) leached Ag from the photocatalysts was determined to be low. Furthermore, *E. coli* suspensions of $\sim 6 \times 10^7$ CFU/mL with Ag^+ concentrations of 1 mg/L have been used to disinfect water, but after 1 h of stirring the final concentration was $\sim 1 \times 10^5$ CFU/mL [56]. Such concentration, which was higher than the one we obtained of leached Ag in our experiments, could not achieve total inactivation of bacteria, thus suggesting that the use of Ag–TiO_2 photocatalysts is advantageous when comparing it to: (a) the activity of TiO_2 (Fig. 6) and, (b) the bactericidal activity observed in literature for the Ag^+ ions [56]. In addition, the use of free silver in solution turns into a risk since its bioaccumulation has shown detrimental impact in the physiology and metabolism in plants [57]. Thus, it is important to focus efforts, such as this study, to attach silver aggregates onto a surface, and of course to sum its bactericidal potential to the photodisinfecting activity of TiO_2. And, (ii) one can expect a decrease in the photoactivity after several uses due to the lost Ag active species on Ag–TiO_2 surface due to their response to light. However, in this case the results showed that after dark processes with the presence of *E. coli* it is possible to regenerate part of the photoactivity since the time needed for total inactivation was 60 min for the used-in-dark Ag(4.3)TiO_2 as well as for the fresh material as observed in Fig. 6. Additional processes to reduce the surface of the photocatalyst may be investigated to regenerate the material.

5. Conclusions

TiO_2 was effectively modified using the hydrothermal synthesis to produce Ag–TiO_2 photocatalyst. Ag loading enhanced the *E. coli* photoinactivation activity of TiO_2 under visible irradiation. Either light source; ultraviolet or Vis, used to evaluate the samples' photoactivity, induced chemical transformations on Ag–TiO_2 that had a remarked effect on its photoactivity. A previous UV pre-irradiation of the Ag–TiO_2 sample led to a total decrease of photoactivity in a subsequent photocatalytic *E. coli* inactivation test under Vis. Such feature was related to the Ag oxidation and Ti^{4+} reduction in TiO_2, thus, reducing the beneficial interaction between Ag^0 and TiO_2, which seems to be responsible of the Vis light photoactivity. In addition, Ag oxidation decreases TiO_2 photoactivity towards the dichloroacetic acid photodegradation due to the consumption of holes to form Ag^+ and Ag^{2+} species during UV irradiation.

Vis light promotes electron transferring processes between Ag^0 and TiO_2 in fresh Ag–TiO_2 leading to the formation of singlet oxygen and hydroxyl radical as determined by EPR spin-trapping experiments. Such species were responsible of total *E. coli* inactivation within short times and low Vis irradiation powers.

Furthermore, post-irradiation events suggest that increased Ag-oxidized states content potentiates the Ag–TiO_2 bacteriostatic action in dark periods leading to *E. coli* inactivation. But also, it was observed that in-dark contact of the oxidized Ag–TiO_2 and *E. coli* possibly promotes recovering of the photocatalyst' Vis light photoactivity lost under UV irradiation.

Acknowledgements

This article is dedicated to the memory of Prof. Aristóbulo Centeno, RIP. Authors wish to present their gratitude to COLCIENCIAS and SENA for financial support (project code: 1102341-19419). C. Castro thanks also to the named Colombian government entities, the UIS, and the EPFL seed-money program: Argentinean-Swiss Cooperation in nanomaterials for bacterial inactivation for financial support to his Ph.D studies. Special acknowledgements to Prof. J. Kiwi and Dr. J. Rengifo-Herrera.

References

[1] O. Carp, C.L. Huisman, A. Reller, Photoinduced reactivity of titanium dioxide, Prog. Solid State Chem. 32 (2004) 33–177.
[2] J.M. Herrman, Heterogeneous photocatalysis: fundamentals and applications to the removal of various types of aqueous pollutants, Catal. Today 53 (1999) 115–129.
[3] C.A. Castro-López, A. Centeno, S.A. Giraldo, Fe-modified TiO_2 photocatalysts for the oxidative degradation of recalcitrant water contaminants, Catal. Today 157 (2010) 119–124.
[4] J. Kiwi, C. Pulgarín, P. Peringer, M. Gratzel, Beneficial effects of heterogeneous photocatalysis on the biodegradation of anthraquinone sulfonate observed in water-treatment, New J. Chem. 17 (1993) 487–494.
[5] Y. Lai, H. Zhuang, C. Lin, A facile method for synthesis of Ag/TiO_2 nanostructures, Mater. Lett. 62 (2008) 3688–3690.
[6] L. Miao, Y. Ina, S. Tanemura, T. Jiang, M. Tanemura, K. Kaneko, S. Toh, Y. Mori, Fabrication and photocromic study of titanate nanotubes loaded with silver nanoparticles, Surf. Sci. 601 (2007) 2792–2799.
[7] W. Zhao, L. Feng, R. Yang, J. Zheng, X. Li, Synthesis, characterization, and photocatalytic properties of Ag modified hollow SiO_2/TiO_2 hybrid microspheres, Appl. Catal. B: Environ. 103 (2011) 181–189.
[8] A. Zielinska, E. Kowalska, J.W. Sobczak, I. Lacka, M. Gazda, B. Ohtani, J. Hupka, A. Zaleska, Silver-doped TiO_2 prepared by microemulsion method: surface properties, bio- and photoactivity, Sep. Purif. Technol. 72 (2010) 309–318.
[9] B. Xin, L. Jing, Z. Ren, B. Wang, H. Fu, Effects of simultaneously doped and deposited Ag on the photocatalytic activity and surface states of TiO_2, J. Phys. Chem. B 109 (2005) 2805–2809.
[10] Y. Liu, C. Liu, Q. Rong, Z. Zhang, Characteristics of the silver-doped TiO_2 nanoparticles, Appl. Surf. Sci. 220 (2003) 7–11.
[11] M.K. Seery, R. George, P. Floris, S.C. Pillai, Silver doped titanium dioxide nanomaterials for enhanced visible light photocatalysis, J. Photochem. Photobiol. A: Chem. 189 (2007) 258–263.
[12] K. Awazu, M. Fujimaki, C. Rockstuhl, J. Tominaga, H. Murakami, Y. Ohki, T. Watanabe, A plasmonic photocatalyst consisting of silver nanoparticles embedded in titanium dioxide, J. Am. Chem. Soc. 130 (2008) 1676–1680.
[13] O. Akhavan, E. Ghaderi, Self-accumulated Ag nanoparticles on mesoporous TiO_2 thin film with high bactericidal activities, Surf. Coat. Technol. 204 (2010) 3676–3683.
[14] D.R. Monteiro, L.F. Gorup, A.S. Takamiya, A.C. Ruvollo, E. Rodrigues, D. Barros, The growing interest of materials that prevent microbial adhesion: antimicrobial effect of medical devices containing silver, Int. J. Antimicrob. Agents 34 (2009) 103–110.
[15] T. Yuranova, A.G. Rincon, C. Pulgarin, D. Laub, N. Xantopoulos, H.J. Mathieu, J. Kiwi, Performance and characterization of Ag-cotton and Ag–TiO_2 loaded textiles during the abatement of *E. coli*, J. Photochem. Photobiol. A: Chem. 181 (2006) 363–369.
[16] H. Zhang, G. Wang, D. Chen, X. Lv, J. Li, Tuning photoelectrochemical performances of Ag–TiO_2 nanocomposites via reduction/oxidation of Ag, Chem. Mater. 20 (2008) 6543–6549.
[17] Y. Tian, T. Tatsuma, Plasmon-induced photoelectrochemistry at metal nanoparticles supported on nanoporous TiO_2, Chem. Commun. 16 (2004) 1810–1811.
[18] K. Kawahara, K. Suzuki, Y. Ohko, T. Tatsuma, Electron transport in silver–semiconductor nanocomposite films exhibiting multicolor photochromism, Phys. Chem. Chem. Phys. 7 (2005) 3851–3855.

[19] H.M. Gong, S. Xiao, X.R. Su, J.B. Hang, Q.Q. Wang, Photochromism and two-photon luminescence of Ag–TiO_2 granular composite films activated by near infrared ps/fs pulses, Opt. Express 15 (2007) 13925–13929.
[20] M.C. Biesinger, L.W. Lau, A.R. Gerson, R.S. Smart, Resolving surface chemical states in XPS analysis of first row transition metals oxides and hydroxides: Sc, Ti, V, Cu and Zn, Appl. Surf. Sci. 257 (2010) 887–898.
[21] Y.E. Nesmelov, D.D. Thomas, Multibore sample cell increases EPR sensitivity for aqueous samples, J. Magn. Reson. 178 (2006) 318–324.
[22] C.I. Zalazar, R.L. Romero, C.A. Martín, A.E. Cassano, Photocatalytic intrinsic reaction kinetics I: mineralization of dichloroacetic acid, Chem. Eng. Sci. 60 (2005) 5240–5254.
[23] M. Kusakabe, Y. Ito, M. Arai, Y. Shirakawa, S. Tamaki, Ionic conductivity in silver-dissolved α-CuI, Solid State Ionics 92 (1996) 135–138.
[24] J. Maier, Physics and Chemistry of Ionic Materials: Ions and Electrons in Solids, John Wiley & Sons, Ltd., London, 2004.
[25] R. Romand, M. Roubin, J.P. Deloume, ESCA studies of some copper and silver selenides, J. Electron. Spectrosc. Relat. Phenom. 13 (1978) 229–242.
[26] B. Xin, Z. Ren, H. Hu, X. Zhang, C. Dong, K. Shi, L. Jing, H. Fu, Photocatalytic activity and interfacial carrier transfer of Ag–TiO_2 nanoparticle films, Appl. Surf. Sci. 252 (2005) 2050–2055.
[27] Z.Y. Huang, G. Mills, B. Hajek, Spontaneous formation of silver particles in basic 2-propanol, J. Phys. Chem. 97 (1993) 11542–11550.
[28] V.K. Kaushik, XPS core level spectra and Auger parameters for some silver compounds, J. Electron. Spectrosc. Relat. Phemon. 56 (1991) 273–277.
[29] O. Akhavan, Lasting antibacterial activities of Ag–TiO_2/Ag/a-TiO_2 nanocomposite thin film photocatalysts under solar light irradiation, J. Colloids Interface Sci. 336 (2009) 117–124.
[30] F. Werfel, O. Brümmer, Corundum structure oxides studied by XPS, Phys. Scr. 28 (1983) 92–96.
[31] H. Gersicher, A. Heller, The role of oxygen in photooxidation of organic molecules on semiconductor particles, J. Phys. Chem. 95 (1991) 5261–5267.
[32] G.A. Ozin, F. Hugues, S.M. Mattar, D.F. McIntos, Low nuclearity silver clusters in fajausite-type zeolites: optical spectroscopy, photochemistry, and relationship to the photodimerization of alkanes, J. Phys. 87 (1983) 3445–3450.
[33] M. Richter, A. Abramova, U. Bentrup, R. Fricke, Proof of reversible Ag^+/Ag^0 redox transformation of mesoporous alumina by in situ UV-Vis spectroscopy, J. Appl. Spectrosc. 71 (2004) 401–403.
[34] R. Konaka, E. Kasahara, W.C. Dunlap, Ultraviolet irradiation of titanium dioxide in aqueous dispersion generates singlet oxygen, Redox Rep. 6 (2001) 319–325.
[35] J.A. Rengifo-Herrera, K. Pierzchala, A. Sienkiewicz, L. Forró, J. Kiwi, C. Pulgarín, Abatement of organics and *Escherichia coli* by N,S co-doped TiO_2 under UV and visible light. Implications of the formation of singlet oxygen ($^1O_2$) under visible light, Appl. Catal. B: Environ. 88 (2009) 398–406.
[36] A. Sienkiewicz, B. Vileno, K. Pierzchala, M. Czuba, P.R. Marcoux, A. Graczyc, P.G. Fajer, L. Forró, Oxidative stress-mediated protein conformation changes: ESR study of spin labeled *Staphylococal nuclease*, J. Phys. Condens. Mater. 19 (2007) 1–13.
[37] K. Sato, K. Takeshita, J.I. Ueda, T. Ozawa, Two reaction sites of a spin label, TEMPOL (4-hydroxy-2,2,6,6-tetramethylpiperidine-N-oxyl), with hydroxil radical, J. Pharm. Sci. 92 (2003) 275–280.
[38] P.K. Robertson, L.A. Lawton, B.J. Cornish, M. Jaspars, Processes influencing the destruction of microcystin-LR by TiO_2 photocatalysis, J. Photochem. Photobiol. A: Chem. 116 (1998) 215–219.
[39] J. Yu, J. Xiong, B. Cheng, S. Liu, Fabrication and characterization of Ag–TiO_2 multiphase nanocomposite thin films with enhanced photocatalytic activity, Appl. Catal. B: Environ. 60 (2005) 211–221.
[40] G. Oliveri, G. Ramis, G. Busca, V. Sanchez, Thermal stability of vanadia–titania catalysts, J. Mater. Chem. 3 (1993) 1239–1249.
[41] M. Logar, B. Jančar, S. Šturm, D. Suvorov, Weak polyon multilayer-assisted in situ synthesis as a route toward a plasmonic Ag/TiO_2 photocatalyst, Langmuir 26 (2010) 12215–12224.
[42] X.S. Li, G.E. Fryxell, C. Wang, M.H. Engelhard, The synthesis of Ag-doped mesoporous TiO_2, Microporous Mesoporous Mater. 111 (2008) 639–642.
[43] S. Buddee, S. Wongnawa, U. Sirimahachai, W. Puetpaibool, Recyclable UV and visible light photocatalytically active amorphous TiO_2 doped with M (III) ions (M = Cr and Fe), Mater. Chem. Phys. 126 (2011) 167–177.
[44] R. Enriquez, P. Pichat, Different net effect of TiO_2 sintering temperature on the potocataytic removal rates of 4-chlorophenol, 4-cholorobenzoic acid and dichloroacetic acid in water, J. Environ. Sci. Health A 41 (2006) 955–966.
[45] A. Romanyuk, P. Oelhafen, Formation and electronic structure of TiO_2–Ag interface, Solar Energy Mater. Solar Cells 91 (2007) 1051–1054.
[46] P.H. Rieger, in: Chapman & Hall (Ed.), Electrochemistry, Chapman & Hall, New York, 1993.
[47] J.A. Rengifo-Herrera, E. Mielczarski, J. Mielczarski, N.C. Castillo, C. Pulgarin, *Escherichia coli* inactivation by N,S co-doped commercial TiO_2 powders under UV and visible light, Appl. Catal. B. Environ. 84 (2008) 448–456.
[48] C.A. Castro, A. Centeno, S.A. Giraldo, Iron promotion of the TiO_2 photosensitization process towards the photocatalytic oxidation of azo dyes under solar-simulated light irradiation, Mater. Chem. Phys. 129 (2011) 1176–1183.
[49] Y. Zhang, K. Aslan, M.J. Previte, C.D. Geddes, Metal-enhanced singlet oxygen generation: a consequence of plasmon enhanced triplet yields, J. Fluoresc. 17 (2007) 345–349.
[50] N.V. Shcherbakov, A.N. Emel'yanov, E.V. Khaula, A.N. Il'ichev, M.V. Vishnetskaya, Y.N. Rufov, Photo- and thermogeneration of singlet oxygen by the metal ions deposited on Al_2O_3 and SiO_2, Russ. J. Phys. Chem. 80 (2006) 918–922.
[51] S. Xu, J. Shen, S. Chen, M. Zhang, T. Shen, Active oxygen species ($^1O_2$, $O_2^{\bullet -}$) generation in the system of TiO_2 colloid sensitized by hypocrellin B, J. Photochem. Photobiol. B: Biol. 67 (2002) 64–70.
[52] T.A. Dahl, Direct exposure of mammalian cells to pure exogenous singlet oxygen ($^1\Delta_gO_2$), Photochem. Photobiol. 57 (1993) 248–254.
[53] Z.Y. Cheng, Y.Z. Li, What is responsible for the initiating chemistry of iron mediated lipid peroxidation: an update, Chem. Rev. 107 (2007) 748–766.
[54] T. Okuno, H. Kawai, T. Hasegawa, H. Ueno, Enhancement of hydroxil radical formation from superoxide anion radical in the presence of organic selenium compounds, J. Health Sci. 47 (2001) 240–247.
[55] E.V. Skorb, L.I. Antonouskaya, N.A. Belyasova, D.G. Shchukin, H. Möhwald, D.V. Sviridov, Antibacterial activity of thin-film photocatalysts based on metal-modified TiO_2 and TiO_2:In_2O_3, Appl. Catal. B: Environ. 84 (2008) 94–99.
[56] Q. Chang, H. He, Z. Ma, Efficient disinfection of *Escherichia coli* in water by silver loaded alumina, J. Inorg. Biochem. 102 (2008) 1736–1742.
[57] Q.S. Xu, J.Z. Hu, K.B. Xie, H.Y. Yang, K.H. Du, G.X. Shi, Accumulation and acute toxicty of silver in *Potamogeton crispus* L., J. Hazard. Mater. 173 (2010) 186–193.